Pharm Res (2015) 32:749–761
DOI 10.1007/s11095-013-1064-x

RESEARCH PAPER

The Cellular Isopeptidase T Deubiquitinating Enzyme Regulates Kaposi's Sarcoma-Associated Herpesvirus K7 Degradation

Jun Xiao • Hui Wu • Lingzhi Peng • Mengdie Chi • Hao Feng

Received: 4 February 2013 / Accepted: 18 April 2013 / Published online: 30 May 2013

ABSTRACT

Purpose To understand the regulated degradation of KSHV K7.

Methods Proteomic screen and immunofluoresence microscopy identified that K7 recruits polyubiquitin chains to membrane fractions; IP and GST pulldown verified the interaction between K7 and Iso T1; Protein stability assay and RQ-PCR demonstrated Iso T1 facilitates K7 degradation.

Results The K7-containing membrane fraction contains a higher level of deubiquitinating (DUB) activity and K7 interacts with a cellular DUB, isopeptidase T1 (Iso T1). Mutational analyses revealed that the ubiquitin-associated domains of Iso T1 are necessary and sufficient to bind K7. Confocal microscopy and fractionation analyses indicated that K7 increases the membrane-associated Iso T1. Furthermore, the knockdown of IsoT1 by shRNA-mediated silencing greatly increased K7 ubiquitination even when proteasome activity was inhibited by lactacystin.

Conclusions IsoT1 disassembles of free ubiquitin chains to facilitate K7 degradation.

KEY WORDS Iso T1 · K7 · KSHV

INTRODUCTION

Kaposi's sarcoma-associated herpesvirus (KSHV, also known as human herpesvirus 8 or HHV-8) is the etiological agent of Kaposi's sarcoma (KS) (1). KSHV infection is also linked to primary effusion lymphoma and multicentric Castleman's diseases, rare lymphoproliferative malignancies of B cell origin (2,3). Genomic sequence indicates that KSHV is a member of gamma-2 herpesviridae that also includes herpesvirus saimiri, rhesus monkey rhadinovirus, and murine herpesvirus 68 (4–6). As an oncogenic DNA virus, the large KSHV genome encodes numerous viral proteins that can stimulate cellular proliferation and trigger inflammatory responses when expressed in mammalian cells (7). Interestingly, both latent and lytic proteins are implicated in the oncogenesis of KSHV-associated malignancies [please see reviews (8,9)]. For example, the KSHV latent vFLIP or K13 and lytic viral G protein-coupled receptor (vGPCR) are oncogenic in a mouse model (10–12). In tissue culture, vGPCR potently activates multiple signaling cascades and downstream transcripition factors, thereby inducing cytokine production and establishing an angioproliferative state to promote cell growth (13,14). Cells expressing vGPCR induce tumor formation in nude mice and vGPCR transgenic mice develop angiogenic lesions resembling human KS (12,14,15). These observations indicate that vGPCR is tumorigenic *in vivo* and suggest that vGPCR is a significant contributor to the sarcomagenesis of KS. Collectively, these findings support the notion that both lytic and latent infections of KSHV play important roles in the pathogenesis of KS.

KSHV K7 is a small membrane protein that is expressed during early reactivation of latently-infected B cells or *de novo* KSHV infection of endothelial cells (16,17). Scientific researchers have shown that K7 targets multiple cellular factors to escape from cellular antiviral apoptosis (17–19). These cellular factors include calcium-modulating cyclophilin ligand (CAML), ubiquitin-like (UBL) and ubiquitin-associated domaincontaining PLIC1, and anti-apoptotic Bcl-2. Interaction with CAML promotes calcium release from the endoplasmic reticulum (ER) and presumably facilitates recovery from apoptotic stimuli (18). Additionally, K7 contains a

J. Xiao · H. Wu · L. Peng · M. Chi · H. Feng (✉)
Key Laboratory of Protein Chemistry and Developmental Biology of Ministry of Education of China, College of Life Science
Hunan Normal University, Changsha, China 410081
e-mail: fenghao@hunnu.edu.cn

Bcl-2 homology domain and a baculovirus inhibitor-of-apoptosis domain that bind Bcl-2 and activated caspase 3, respectively, thereby impeding caspase-dependent apoptosis (17). Finally, K7 interacts specifically with the highly conserved UBA domain of PLIC1 that otherwise sequesters polyubiquitinated proteins from the proteasome, leading to the rapid degradation of IκB and p53 (19). These findings clearly established anti-apoptotic activity of K7 in mammalian cells and are inferred to prevent cellular antiviral activities. Yet, the roles of K7 in KSHV infection remain obscure. Recently, we have discovered that K7 binds KSHV vGPCR and induces its proteasomal degradation (20). Interestingly, K7 significantly reduces vGPCR tumorigenicity in nude mice, implying that the protein expression of K7 and vGPCR is important for KSHV-associated malignancies. Thus, understanding the mechanisms governing K7 and vGPCR protein expression will shed light on KSHV pathogenesis.

Regulated protein degradation plays important roles for a number of fundamental biological processes including viral replication. In higher eukaryotes, proteins are degraded either by the ubiquitin-proteasome system (UPS) or the lysosome. For UPS substrates, proteins destined for destruction are tagged with ubiquitin through concerted actions of the E1 activating enzyme, E2 conjugating enzyme, and E3 ligase (21). Conversely, polyubiquitin chains can be "edited" by DUB enzymes (such as Ubp6) to slow down protein degradation (22). Polyubiquitinated proteins are then transferred to the proteasome in which proteolytic degradation occurs. While proteasomal substrates are degraded, ubiquitin chains are disassembled to replenish the free ubiquitin pool. Presumably, timely disassembly of free polyubiquitin chains also prevents potential competitive binding to proteasomal subunits that otherwise serve as acceptors for polyubiquitinated proteins, thereby facilitating the ubiquitin/proteasome-depdendent proteolysis (23). Isopeptidase T1 [Iso T1, also known as ubiquitin-specific-processing protease (USP) 5] is the major DUB that disassembles free polyubiquitin chains *in vitro* (24). Indeed, the yeast homolog of Iso T1, Ubp14 is essential for normal ubiquitin recycling and proteasomal degradation of a model substrate, ub-P-βgal (23). Knockout of Ubp14 results in an accumulation of free ubiquitin chains and inhibits ub-P-βgal degradation, supporting the possibility that free ubiquitin chains compete for binding to proteasome. However, overexpression of Ubp14 also inhibits ub-P-βgal degradation, suggesting that Ubp14 has unrecognized function in proteasome-mediated proteolysis (23).

Herein, we have identified the deubiquitinatination at which K7 targets a cellular DUB, Iso T1, to modulate ubiquitin catabolism. It was found that K7 interacts with the UBA domains of Iso T1 and increases its membrane localization, thereby inducing an accumulation of free ubiquitin chains. The knockdown of Iso T1 and overexpression of Iso T1 enzyme dead mutant significantly block K7 degradation. Interestingly, knockdown of Iso T1 results in an accumulation of polyubiquitinated K7 when the proteasome is inhibited. Our study supports the conclusion that K7 recruits cellular Iso T1 to ER membrane, where Iso T1 disassembles of free ubiquitin chains to facilitate K7 degradation.

MATERIALS AND METHODS

Cell Culture and Transfection

HEK293T (293T), HeLa, and human endothelial ECV cells were bought from American Typical Collection Center (ATCC) and grown in DMEM supplemented with 10% fetal bovine serum, 2 mM L-glutamine, 100 U/ml penicillin, and 100 μg/ml streptomycin. BJAB/T-Rex_FRT or BJAB/T-Rex_K7 cells were grown in RPMI 1640 supplemented with 10% fetal calf serum, 5 mM L-glutamine, 100 U/ml penicillin, and 100 μg/ml streptomycin. HeLa cells were transfected with Fugene 6, 293T cells were transfected with calcium phosphate (Clontech), and ECV cells were transfected with lipofectamine 2000 (Invitrogen). The stable HEK293/T-Rex and BJAB/T-Rex inducible cell lines were maintained with 100 and 200 μg/ml hygromycin, respectively, and induced with 1 μg/ml of doxycycline as previously described (25).

Plasmids

If not specified, all constructs are derived from pcDNA5/FRT/TO (Invitrogen). Plasmids containing K7 and K7 mutants were described elsewhere (18,19). Iso T1 and USP6 were amplified by PCR and inserted into pcDNA5/FRT/TO that contains either a Flag epitope or an HA epitope using BamHI and XhoI. Iso T1 mutant lacking UBAI, UBAII, or UBAI+II were constructed using overlapping PCR primers and cloned into pcDNA5/FRT/TO similarly. The UBAI [amino acid (aa) 633–671], UBAII (aa 702–736), and UBAI+II (aa 633–736) were PCR amplified and cloned into pGEX-4T-1 (Promega) between BamHI and XhoI sites. The plasmid containing GST-PLIC1(382–589) used as a positive control was described previously (19).

Immunoprecipitation and Immunoblot

Immunoprecipitation and immunoblot were performed as previously described (18,26). Briefly, centrifuged whole cell lysates were precleared with protein A/G agarose for 90 min at 4°C. Antibody (up to 2 μg) was added to the supernatant and the mixture was incubated at 4°C up to

12 h, after which, 20 µl of protein A/G agarose was added and incubation was further extended for another hour. After extensive washing, precipitated proteins were resolved by SDS-PAGE and analyzed by immunoblot.

Immunoblot detection was performed with anti-V5 antibody (1:5000, Invitrogen), anti-Flag M2 antibody (1:5000, Sigma), anti-HA (1:2000, Covance), anti-PDI (1:3000, Calbiochem.), anti-calreticulin (1:3000, Bethyl Group), or anti-actin (1:30,000, Abcam) separately. Proteins were visualized with chemical luminescent detection reagent (Pierce) and a Fuji LAS-3000 camera.

Immunofluorescence Microscopy

HeLa cells were fixed with paraformaldehyde and permeabilized with Triton X-100 [0.2% in phosphate buffered saline (PBS, 137 mM NaCl, 2.7 mM KCl, 10 mM Na2HPO4, 2 mM KH2PO4, pH7.4)]. After stained with primary and secondary antibodies, cells were analyzed by immunofluorescence microscopy as previously described (26). For commercial antibodies, mouse monoclonal anti-Flag antibody (1:1000), rabbit polyclonal anti-Flag antibody (1:400, Sigma), anti-PDI (1:200, Calbiochem.), mouse monoclonal anti-V5 antibody (1:500, Invitrogen), anti-HA (1:200, Covance) were used. All conjugated secondary antibodies were obtained from Molecular Probes and diluted at 1:1000 (Alexa 488-conjugated) or 1:500 (Alexa 568-conjugated).

Protein Purification and GST Pulldown Assay

GST or GST fusion proteins containing the UBAI, UBAII, UBAI+II domains of Iso T1, or PLIC1(382–589) were expressed and purified as previously described (19,26). Briefly, BL21 cells carrying plasmids expressing GST or GST fusion proteins were induced with 1 mM Isopropyl β-D-1-thiogalactopyranoside for 2 h. Proteins were solubilized in PBS containing 0.1% sarcosyl and 1% Triton X-100, supplemented with protease inhibitor cocktail. Glutathione sepharose resin was added to centrifuged supernatant and incubated at 4°C for 1 h. After extensive washing, protein bound resin was either directly used for GST pulldown assays or stored at −20°C for future experiments.

GST pulldown assays were performed as previously described (19,26). Briefly, 293T cells transfected with plasmid containing K7 were lysed with NP40/Triton X-100 buffer (150 mM NaCl, 50 mM Tris.HCl, pH7.4, 5 mM EDTA, 1% NP40, 1% Triton X-100) supplemented with protease inhibitor cocktail. Centrifuged supernatant was mixed with protein-loaded glutathione resin and the mixture was incubated at 4°C for 2 h. After extensive washing, protein was eluted with SDS-PAGE loading buffer at 95°C for 5–10 min and analyzed by immunoblot.

Protein Stability

Transiently transfected ECV cells were pulse labeled with ^{35}S-methionine/cysteine (Met/Cys) for 30 min. After extensive washing with PBS, cells were chased with regular medium up to 16 h. At various time points, cells were harvested, washed with cold PBS, resuspended in RIPA buffer (50 mM Tris–HCl [pH7.4], 150 mM NaCl, 0.5% sodium deoxycholate, 0.1% SDS, 1% NP40, 5 mM EDTA/EGTA), and lysed by passing through a 26-G syringe 15 times. Centrifuged supernatant was pre-cleared with protein A/G agarose and then mixed with 2 µg of anti-Flag M2 antibody. Incubation was carried out at 4°C for 4–6 h. Protein A/G agarose was added and incubation was further extended for up to 90 min. After extensive washing with RIPA buffer, precipitated proteins were resolved by SDS-PAGE, and analyzed by autoradiography. The relative intensity of both K7 protein bands was quantified using phosphorimager to obtain a composite degradation curve.

Intracellular Fractionation

BJAB/T-Rex or HEK293/T-Rex cells were harvested, washed with ice-cold PBS, and resuspended with hypotonic buffer (10 mM Tris; 250 µM sucrose; 20 mM HEPES, pH 7.4; 0.2 mM EDTA) supplemented with 1 mM DTT and protease inhibitor cocktail. The suspension was incubated on ice for 15 min and lysed with a homogenizer for 25 strokes. Nuclei and unbroken cells were removed by centrifugation at 700×*g* for 15 min. The supernatant was collected and centrifugation was repeated once. The supernatant at this point is regarded as whole cell lysate and subjected to centrifugation at 16,000×*g* for 30 min. The pellet was then resuspended with hypotonic buffer and supernatant was transferred to a new tube. Both supernatant and resuspended pellet were centrifuged at 16,000×*g* for 15 min; this process was repeated twice to obtain the membrane fraction (pellet) and cytosolic fraction (supernatant). The protein fractions were then analyzed by immunoblot or used for *in vitro* deubiquitination assays (the membrane fraction only).

Knockdown of Iso T1 and Real Time PCR

Five plasmids (pLKO.puro) expressing shRNA targeting Iso T1 and the control plasmid expressing a scrambled shRNA were purchased from Sigma. Plasmids were transfected into ECV cells to transiently knock down Iso T1 expression. Alternatively, transfected cells were selected with puromycin (1 µg/ml) to establish stable cell lines and multiple colonies were pooled for quantification of knockdown efficiency by real time PCR.

For real time PCR, total RNA was extracted with Trizol according to manufacturer's protocol (Invitrogen). The

primers were designed using Primer Express v1.5 (Applied Biosystems). The efficiency and specificity of the primers were validated and real-time PCR using cDNA was performed with an ABI 7500 sequence detection system (Applied Biosystems).

Deubiquitination Assay

The *in vitro* deubiquitination assay was performed as previously described (27). Briefly, 10 µg of the membrane fraction isolated as described above was incubated with 1 µg of tetra-ubiquitin substrate (Affinity Research Products) in 20 µl of 50 mM Tris–HCl (pH7.2) containing 1 mM dithiothreitol (DTT) for 2 h at 37°C. Reaction mixtures were analyzed by SDS-PAGE, followed by silver staining or coommassie staining and immunoblot with a mouse monoclonal antibody against ubiquitin (P4D1, Santa Cruz).

RESULTS

K7 Induces an Accumulation of Free Ubiquitin Chains in the Membrane Fraction

It has been shown that K7 protein is regulated by the UPS degradation pathway (19). While K7 induces vGPCR degradation (20), K7 protein expression is greatly increased by vGPCR (unpublished data). These findings suggest that K7 protein is dynamically regulated during KSHV replication. To further understand molecular mechanisms by which K7 is degraded, we employed a proteomic screen to identify proteins enriched in the K7-containing membrane fraction. The membrane fractions from BJAB/T-Rex_FRT (BJAB/FRT) and BJAB/T-Rex_K7 (BJAB/K7) cells were resolved by isoelectric focusing and SDS-PAGE. Proteins differentially displayed were selected for mass spectrometry analysis (Fig. 1). Two peptides of an 8 kDa candidate protein matching ubiquitin were identified, suggesting that K7 expression induces an accumulation of ubiquitin in the membrane fraction (Fig. 1).

To test whether K7 induces an accumulation of ubiquitin chains in the membrane fraction, total protein of 50 µg (whole cell lysate) or 10 µg (the membrane fraction) was analyzed by coommassie staining and immunoblot with P4D1 anti-ubiquitin antibody. This revealed that there was a substantially higher level of ubiquitin in the membrane fraction of BJAB/K7 cells than in that of BJAB/FRT cells, supporting the notion that K7 induces an accumulation of ubiquitin in the membrane fraction (Fig. 2a). Surprisingly, the size of these proteins corresponds to a monomer, dimer, trimer, tetramer, and oligomers of ubiquitin, suggesting that these proteins are free (unanchored) ubiquitin or polyubiquitin chains. In agreement with this possibility, immunoblot analysis using antibody

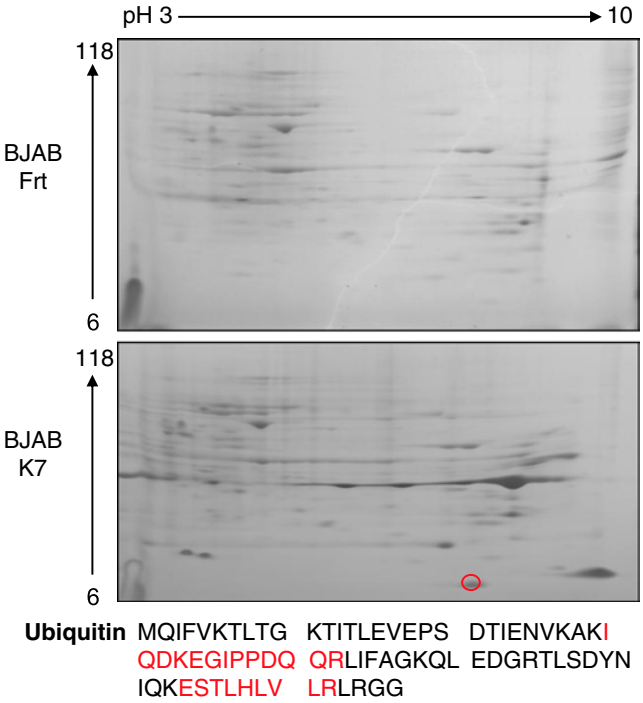

Fig. 1 Identification of ubiquitin accumulated in the membrane fraction of BJAB/K7 cells. The membrane fractions of BJAB/FRT cells and BJAB/K7 cells were resolved by two-dimensional gel electrophoresis. Proteins differentially displayed were excised and subjected to mass spectrometry analysis. Two peptides matching ubiquitin were identified and highlighted in *red* (*bottom*).

(FK2) reacting specifically with polyubiquitinated proteins did not yield significant difference between the two membrane fractions (Fig. 2, right panel). Ubiquitin localizes predominantly in the cytosol or nucleus; the fact that K7 increases membrane localization of ubiquitin suggests that K7 alters its intracellular distribution. This possibility was examined by indirect immunofluorescent microscropy with transiently transfected HeLa cells. In HeLa cells, ubiquitin distributed throughout the entire cytoplasm with a more concentrated perinuclear localization. Upon K7 expression, ubiquitin displayed a more punctate pattern that also includes a diffused perinuclear region (Fig. 2b). The punctate intracellular structures are positive for both ubiquitin and K7, indicating that these two proteins co-localize to intracellular compartments. This observation supports the conclusion that K7 alters ubiquitin intracellular distribution and suggests that K7 may interact with these ubiquitin chains.

It has been shown that K7 interacts with multiple components of the UPS system including cellular PLIC1 and the proteasome substrate, vGPCR (19,20). The observation that K7 induces accumulation of ubiquitin chains in the membrane fraction prompted us to test whether K7 associates with these ubiquitin chains. 293T cells were transfected with a plasmid containing either the wt K7 or the 5K>R mutant (all lysine residues changed to arginine). The 5K>R mutant

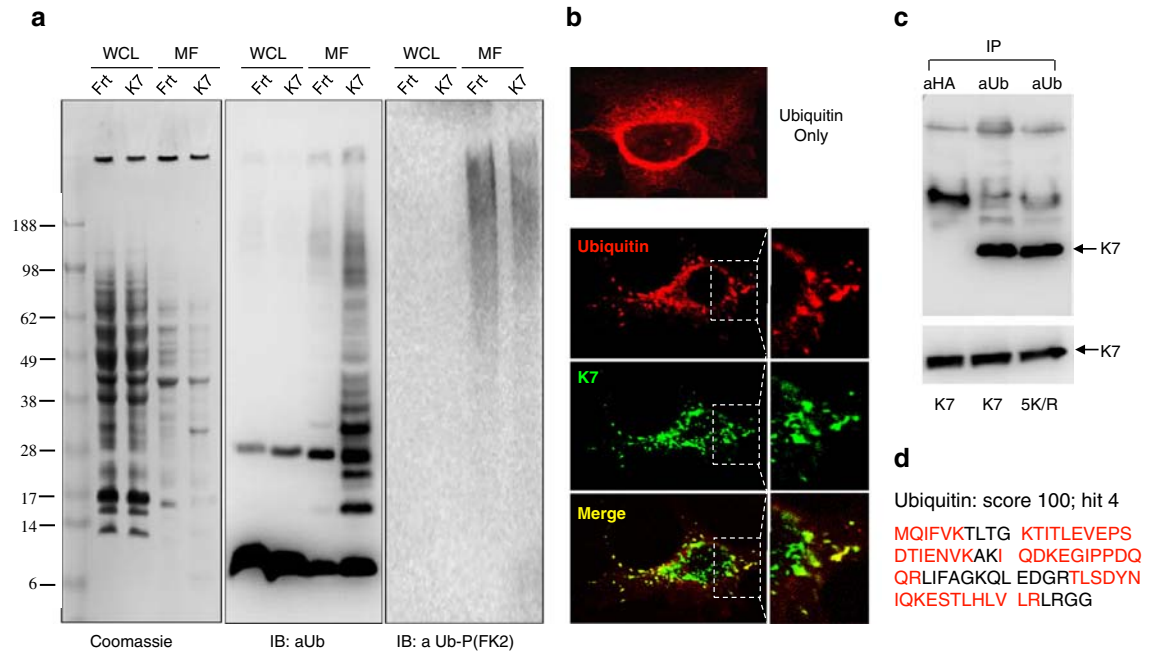

Fig. 2 K7 induces an accumulation of polyubiquitin chains in the membrane fraction. (**a**) K7-induced ubiquitin accumulation analyzed by immunoblot. Whole cell lysates (WCL, 50 μg) and the membrane fractions (MF, 10 μg) from BJAB/FRT or BJAB/K7 cells were resolved by SDS-PAGE, followed by coommassie staining (*left panel*), immunoblot analysis using anti-ubiquitin (P4D1) (*middle panel*) or FK2 (*right panel*). *Numbers on the left* indicate protein standards in kilodalton. *Note*, K7 is not detected by immunoblot analysis. (**b**) K7 co-localizes with ubiquitin. HeLa cells were transfected with a plasmid containing HA-ubiquitin alone or with a plasmid containing K7-V5. Cells were stained with anti-HA and FITC-conjugated anti-V5 antibodies. *Images at the right* represent an enlarged (2-fold) view of the boxed regions. Representative sections and their overlay are shown. (**c**) K7 associates with ubiquitin by co-immunoprecipitation. 293T cells were transfected with a plasmid containing V5-tagged wt K7 or the 5K>R mutant. At 36 h post-transfection, centrifuged whole cell lysates were precipitated with anti-ubiquitin (P4D1). Precipitated proteins (*top panel*) and whole cell lysates (*bottom panel*) were analyzed by immunoblot with anti-V5 antibody. Anti-HA antibody was included as a negative control. (**d**) Identification of ubiquitin as a K7-interacting protein. K7 binding proteins were purified by anti-Flag agarose resin and identified by mass spectrometry. Peptide sequences matching to ubiquitin were highlighted in *red* and the score is indicated.

which can not be ubiquitinated was included as a control to rule out the possibility that K7 is precipitated by covalently conjugated ubiquitin chains. Whole cell lysate was centrifuged and precipitated with P4D1 antiubiquitin antibody. Indeed, we found that K7 was readily detected in immunocomplexes precipitated by anti-ubiquitin antibody, but not by anti-HA antibody, indicating an interaction between K7 and ubiquitin chains (Fig. 2c). Of note, the K7 species precipitated by the P4D1 anti-ubiquitin antibody correspond to K7 without ubiquitination and the 5K>R mutant is equally precipitated. Furthermore, ubiquitin and its precursor were identified as K7-binding proteins by affinity purification and mass spectrometry analysis (Fig. 2d). Taken together, these findings collectively support the conclusion that K7 modulates intracellular ubiquitin metabolism.

Evidence that K7 Recruits a Deubiquitinating Enzyme (DUB) to the Membrane Fraction

The fact that K7 induces an accumulation of ubiquitin chains in the membrane fraction indicates altered catabolism of ubiquitin chains and suggests that K7 deregulates the dissembly of free polyubiquitin chains. One possible scenario is that K7 increases DUB activity in the membrane fraction in order to affect deubiquitination and subsequent protein degradation. To test this, an *in vitro* deubiquitination assay was performed to assess the membrane-associated DUB activity. Tetraubiquitin was used as a substrate and 10 µg of total membrane proteins were added. As expected, there was significantly less of the tetra-, tri-, and di-ubiquitin that were converted into ubiquitin monomers, in the reaction containing the membrane fraction derived from BJAB/K7 cells (Fig. 3, left panel). Silver staining also supports this observation and confirms that the same amount of membrane proteins was added (Fig. 3, right panel). This result indicates that there is more DUB activity associated with the membrane fraction of BJAB/K7 cells than that of BJAB/FRT cells. This further implies that K7 recruits a DUB(s) to the intracellular membrane.

K7 Interacts with the UBA Domains of Iso T1

Our data from fractionation and *in vitro* deubiquitination assays support the possibility that K7 expression increases the membrane localization of a cellular DUB(s). Thus, we explored the possibility that K7 interacts with a cellular

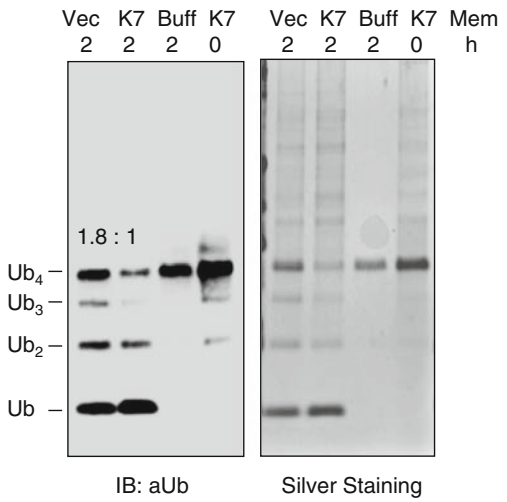

Fig. 3 The membrane fraction from BJAB/K7 contains a higher level of deubiquitinating enzyme activity than the control. Ten μg of the membrane fractions of BJAB/K7 or BJAB/FRT cells were used for an *in vitro* deubiquitination assay with tetraubiquitin as a substrate. Reaction mixtures were analyzed by SDS-PAGE, followed by immunoblot with anti-ubiquitin (P4D1, *left panel*) or by silver staining (*right panel*). Mem: membrane fraction. *Numbers on left panel* indicate the relative intensity of remaining tri- and tetraubiquitin.

DUB(s). There are approximately 95 DUBs annotated in the human genome, but only two contain UAB domains with which K7 interacts (28). These two DUBs include Iso T1 (also known as USP5) and Iso T3 (also known as USP13). While the function of Iso T3 remains unknown, Iso T1 and its yeast homolog Ubp14 are major cytosolic DUBs that disassemble free polyubiquitin chains (23,24). Interestingly, knockout of Ubp14, the yeast homolog of Iso T1, results in an accumulation of free polyubiquitin chains. Thus, we examined whether K7 deregulates cellular Iso T1.

Initially, we assessed a possible interaction between K7 and Iso T1 by a coimmunoprecipitation (co-ip) assay. 293T cells were transfected with plasmids containing K7-V5 and Flag-Iso T1 or Flag-USP6. The USP6 serves as a control as it does not contain a UBA domain. We found that K7 was precipitated by anti-Flag antibody in the presence of Flag-Iso T1, but not of Flag-USP6 (Fig. 4a). This result supports a specific interaction between K7 and Iso T1 and also suggests that K7 interacts with Iso T1 *via* the UBA domains. Iso T1 contains two putative UBA domains that are situated within its internal region (aa 633–736), designated UBAI and UBAII (diagrammed in Fig. 4b) (23). To assess the contribution of these two UBA domains to the interaction between Iso T1 and K7, Iso T1 mutants that lack the UBAI, UBAII, or UBAI+II were constructed and used for a co-ip experiment. The assay revealed that the deletion of UBAII, but not UBAI, abolished the interaction of Iso T1 with K7 (Fig. 4b). Moreover, deletion of both UBA domains also abrogated this interaction, consistent with the importance of the UBAII domain. These results indicate that UBAII is necessary for Iso T1 to bind K7.

It has been shown that the UBA domain of PLIC1 is sufficient to interact with K7 (19), therefore we examined whether the UBA domains of Iso T1 also interact with K7. The UBAI, UBAII, and UBAI+II domains were expressed and purified from E.coli as GST fusion proteins. Whole cell lysate of 293T cells, transfected with a plasmid containing K7-Flag, was mixed with glutathione resin loaded with either GST or GST fusion proteins. K7, recovered by GST fusion proteins, was analyzed by immunoblot with anti-Flag antibody. Interestingly, it was found that both UBA domains (UBAI+II) are necessary to interact with K7, but neither the UBAI domain, nor the UBAII domain is able to independently interact with K7 (Fig. 4c). However, it is possible that K7 interacts with UBAII and the UBAI is necessary to allow proper folding of UBAII when it is expressed as a GST fusion protein (Fig. 4c). Furthermore, the UBAI+II was able to recover significantly higher amount of K7 than the GST-PLIC1(382–589). As the UBAI and UBAII domains are relatively small (39 and 35 aa, respectively) and the GST fusion proteins containing these UBA domains did not show significant size difference (Fig. 4c, lane 1, 2, and 3 of bottom panel), the AU1 (DTYRYI) epitope was inserted downstream of UBAI and UBAII domains. Immunoblot analysis using anti-AU1 antibody indicated that these fusion proteins were correctly expressed (Fig. 4c, middle panel). Taken together, these data conclude that K7 interacts with Iso T1 *via* its UBA domain(s).

K7 Deregulates Cellular Iso T1

The membrane fraction of BJAB/K7 cells contains more DUB activity than that of BJAB/FRT cells, suggesting the recruitment of Iso T1 by K7. This notion is consistent with the observed interaction between K7 and Iso T1. Given that K7 is a transmembrane protein, we examined whether Iso T1 also localizes to intracellular membrane structures (such as the ER) in the presence of K7. HeLa cells were transfected with plasmids containing Flag-Iso T1 or K7-V5, fixed and then subjected to immunofluorescent microscopy. While Iso T1 distributed throughout a cell with primary localization in the nucleus, K7 showed more punctate staining in the cytoplasm (Fig. 5a). Because Iso T1 is highly expressed and resides in the cytosol and nucleus (Fig. 5a), cells were permeabilized and washed extensively with PBS before fixation to remove cytosolic/nuclear Iso T1. This approach permits the detection of membrane-associated Iso T1 by confocal microscopy. Iso T1 has an intracellular pattern of membrane structures similar to that stained by anti-V5 antibody for K7, supporting that K7 recruits Iso T1 to the membrane fraction (Fig. 5b). In the absence of K7, there was a minimal level of Iso T1 associated with membrane after extensive washing (data not shown). This further emphasizes that K7 is responsible for the membrane association of Iso T1.

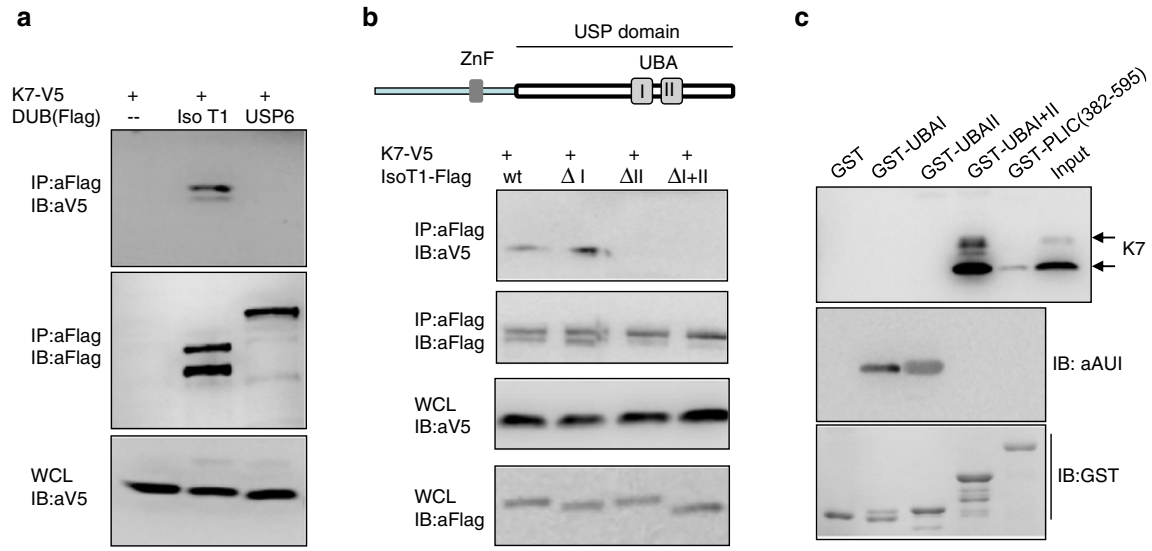

Fig. 4 K7 interacts with cellular isopeptidase T1 (Iso T1) deubiquitinating enzyme. (**a**) K7 interacts with Iso T1 by co-immunoprecipitation. 293T cells were transfected with plasmids containing V5-tagged K7 and Flag-tagged Iso T1 or USP6. At 36 h posttransfection, cells were harvested and centrifuged cell lysates were subjected to precipitation with anti-Flag antibody. Precipitated proteins were analyzed by immunoblot with anti-V5 (K7, *top panel*) or anti-Flag (*middle panel*). Whole cell lysates were analyzed by immunoblot with anti-V5 (*bottom panel*). (**b**) The second UBA domain of Iso T1 is important for its interaction with K7. Plasmids containing wt Iso T1 or Iso T1 mutants with deletions of the first UBA (ΔUBAI), the second UBA (ΔUBAII), or both (ΔUBAI+II), together with a plasmid containing K7-V5, were transfected into 293T cells. Co-immunoprecipitation and immunoblot were performed as in (**a**). Precipitated proteins were analyzed by immunoblot with anti-V5 (K7, *top panel*) or anti-Flag (2nd panel from *top*). Whole cell lysates were analyzed by immunoblot with anti-Flag (3rd panel from *top*) and anti-V5 (*bottom panel*) antibodies. USP: ubiquitin-specifc-processing protease. ΔI, deletion of UBAI; ΔII, deletion of UBAII; ΔI+II, deletion of UBAI+II. (**c**) The UBA domains of Iso T1 are sufficient to interact with K7. GST or GST fusion proteins containing PLIC1(382–589), UBAI, UBAII, or UBAI+II were used for an *in vitro* GST pulldown assay. Proteins recovered by protein-loaded glutathione sepharose were analyzed by immunoblot with anti-V5 (K7, *top*) and anti-AU1 (GST-UBAI or UBAII, *middle*), or by coommassie staining (GST proteins, *bottom*).

To further corroborate the data from confocal microscopy, HEK293/T-Rex cells were transfected to establish a HEK293/T-Rex_HA-Iso T1 cell line in which Iso T1 expression is induced with doxycycline as previously described (25). After Iso T1 expression was confirmed (Fig. 5c), HEK293/T-Rex_HA-Iso T1 cells were transfected with a plasmid containing K7-Flag and induced with doxycycline (1 μg/ml). At 36 h post-transfection, cells were harvested and subjected to intracellular membrane fractionation. Whole cell lysate was centrifuged to obtain the membrane fraction and cytosolic fraction. Whole cell lysates, the membrane fraction, and cytosolic fraction were analyzed by immunoblot with anti-PDI, anti-actin, and anti-Flag (K7). K7 was previously shown to localize in both the mitochondrion and ER compartment (17,18). In agreement with our data from confocal microscopy, K7 consistently increased the amount of Iso T1 in the membrane fraction, despite the fact that Iso T1 is predominantly a cytosolic protein (Fig. 5d).

Iso T1 is Important for K7 Degradation

It has been shown that K7 is a proteasome substrate and its protein expression is determined largely by posttranslational degradation (19). Recently, we have found that K7 interacts with vGPCR and induces its proteasome-dependent degradation (20). Our findings revealed that both vGPCR and K7 are proteasome substrates whose protein expression is regulated by the UPS system. Iso T1 is one of the major cytosolic DUBs at which multiple protein degradation pathways converge. We reasoned that alteration of Iso T1 expression likely impacts the regulated degradation of K7.

To examine the roles of Iso T1 in K7 protein degradation, we employed both shRNA-mediated knockdown and overexpression of the enzyme dead mutant of Iso T1, Iso T1C335S. Among five shRNA molecules tested, two shRNA had significant effect in reducing Iso T1 expression by transient transfection assay and real time PCR analysis. In particular, the shRNA #1 and #4 had similar knockdown efficiency of approximately 50% by immunoblot analysis and of 60% by real time PCR, respectively (Fig. 6). Next, K7 protein expression was examined by immunoblot under conditions of Iso T1 knockdown or overexpression of the enzyme dead mutant. Knockdown of Iso T1 significantly increased K7 protein expression, with the shRNA #4 showing more pronounced effect (Fig. 7a). It has been indicated that K7 protein level is regulated by degradation (19), therefore a pulse chase experiment was performed to examine the role of Iso T1 in K7 degradation. Indeed, Iso T1 knockdown by shRNA silencing greatly inhibited K7 degradation (Fig. 7b). Furthermore, overexpression of the Iso T1 C335S enzyme dead mutant dramatically promoted K7 protein expression and inhibited K7 protein degradation (Fig. 7a and c). Presumably, the Iso

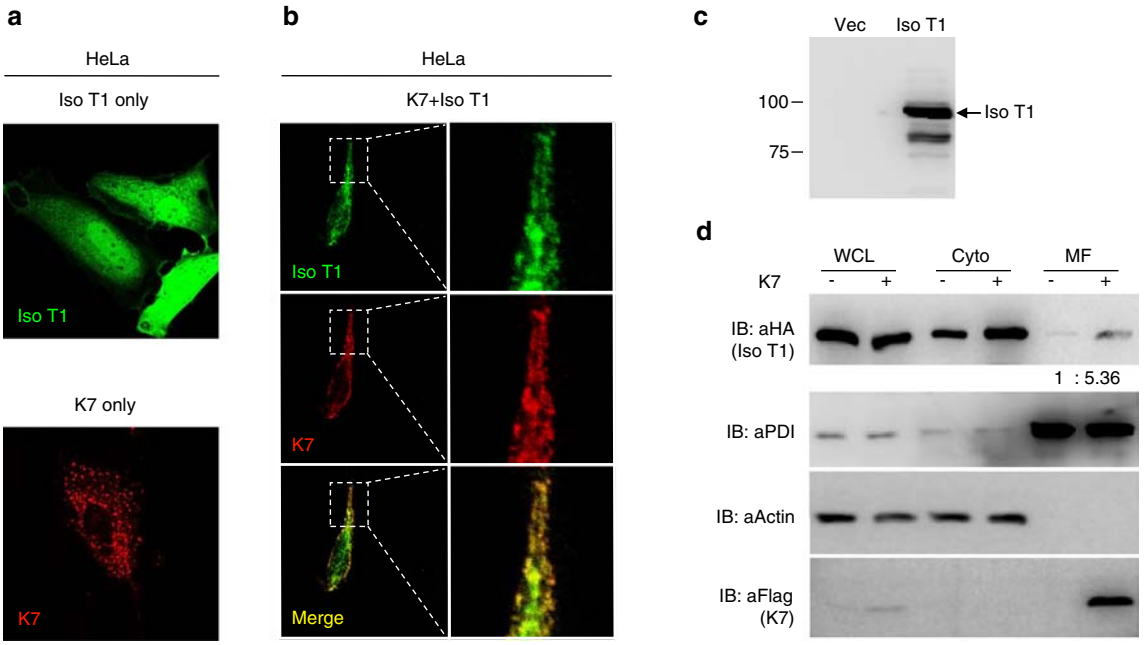

Fig. 5 K7 recruits Iso T1 to the intracellular membrane. (**a**) Distinct intracellular localization of Iso T1 and K7. HeLa cells transfected with plasmids containing either Flag-Iso T1 or K7-V5. At 16 h post-transfection, cells were fixed and stained with rabbit anti-Flag (*top panel*) or mouse anti-V5. One representative section is shown. (**b**) Intracellular colocalization of Iso T1 and K7. HeLa cells transfected with plasmids containing Flag-Iso T1 and K7-V5 were permeabilized with 0.2% triton X-100, and then washed extensively with PBS to remove cytosolic Iso T1. Cells were fixed and stained with rabbit anti-Flag and mouse anti-V5. Representative sections and their overlay are shown. Images at the right represent an enlarged (3-fold) view of the boxed regions. Representative sections and their overlay are shown. (**c**) Induced expression of Iso T1 in HEK293 cells. Stable HEK293/T-Rex_HA-Iso T1 (Iso T1) cells or vector (Vec) cells were induced with doxycycline (1 μg/ml) for 36 h. Whole cell lysate was analyzed by immunoblot with anti-HA antibody. (**d**) K7 increases Iso T1 membrane localization by fractionation. HEK293/T-Rex_HA-Iso T1 were transfected with a plasmid containing K7-Flag and induced with doxycycline (1 μg/ml). At 36 h post-transfection, cells were harvested and subjected to intracellular fractionation. Whole cell lysate (WCL), the membrane fraction (MF), and cytosolic fraction (Cyto) were obtained and analyzed by immunoblot with anti-HA (Iso T1, *top panel*), anti-PDI (*2nd panel*), anti-β-actin (*3rd panel*), and anti-Flag (K7, *bottom panel*). *Numbers below the top panel* indicate relative intensity of the Iso T1 protein.

T1C335S mutant functions as a dominant negative of the wt Iso T1 and other closely related DUBs. Collectively, these findings indicate that Iso T1 is a critical component of the UPS system that regulates K7 protein degradation.

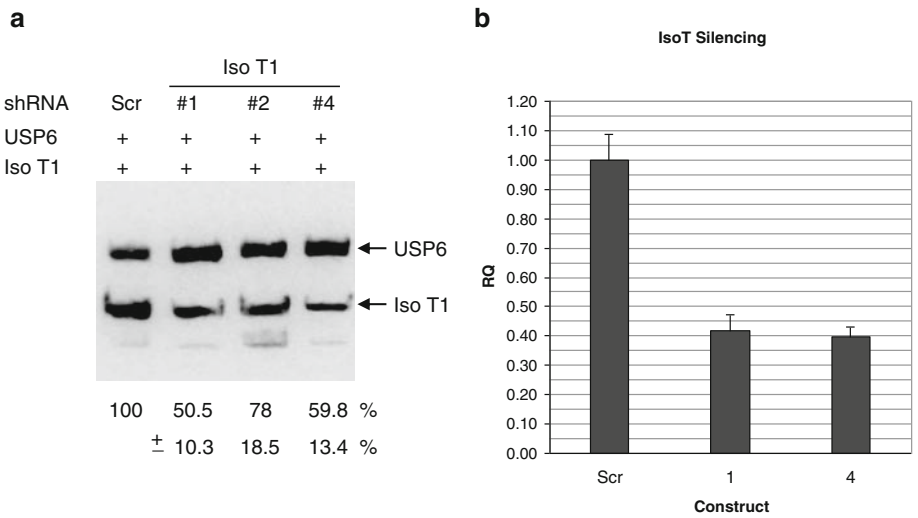

Fig. 6 Knockdown of Iso T1 by shRNA-mediated silencing. (**a**) Knockdown of Iso T1 by transient transfection. 293T cells were transfected with plasmids as indicated. At 48 h post-transfection, whole cell lysates were analyzed by immunoblot with anti-Flag antibody. *Numbers* indicate the relative intensity of Iso T1 band that was normalized to USP6 band. Data represents three independent experiments and numbers at the bottom denote mean (*top row*) and standard deviation (*bottom row*). *Scr* scrambled shRNA. (**b**) Knockdown of Iso T1 by real time PCR. Stable ECV cells carrying pLKO.puro, pLKO.Iso T1shRNA#1, or pLKO.Iso T1shRNA#4 were collected for total RNA extraction and real time PCR analysis. *RQ* relative quantity.

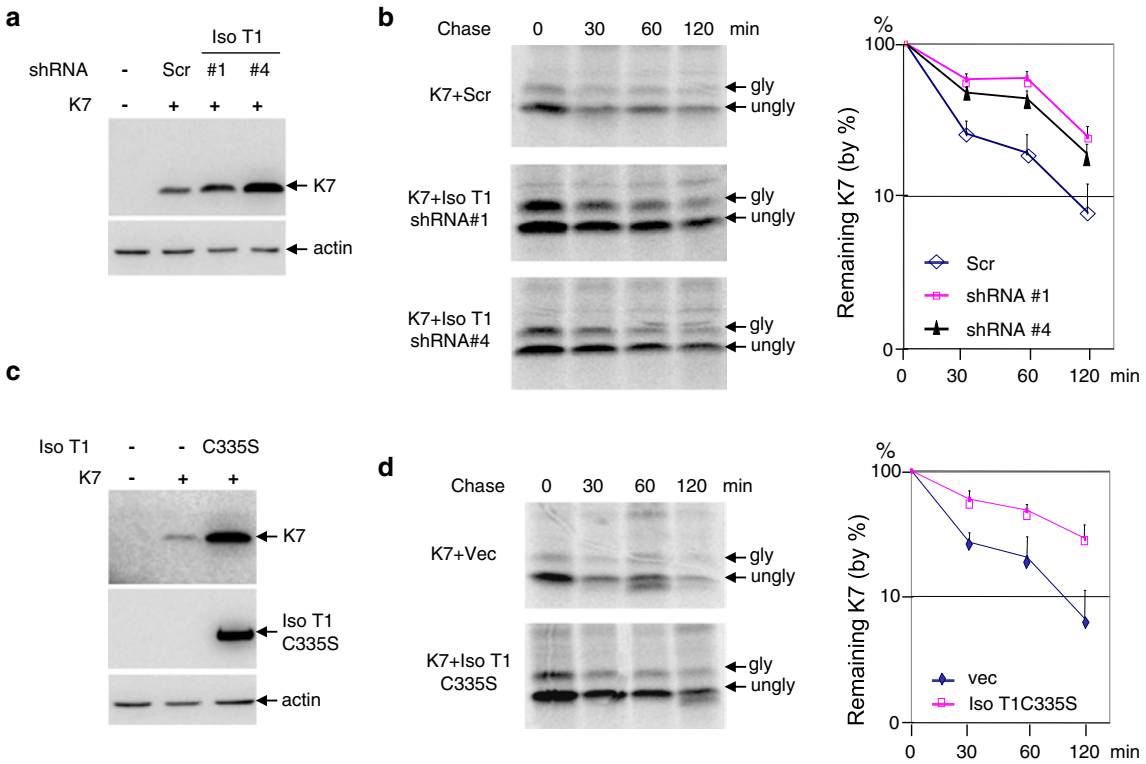

Fig. 7 Iso T1 is important for K7 degradation. (**a**) Knockdown of Iso T1 increases K7 protein expression. ECV cells were transfected with plasmids as indicated. At 36 h posttransfection, whole cell lysates were analyzed by immunoblot with anti-Flag (K7, *top panel*) or anti-actin (*bottom panel*). (**b**) Knockdown of Iso T1 inhibits K7 degradation. ECV cell transfected with plasmids as indicated (on the *left*) were pulse labeled with [35S]-methionine/cysteine mix and chased up to 2 h. Anti-Flag precipitated K7 was analyzed by autoradiography (*left panels*) and K7 proteins (both bands) were quantified using phosphorimager (*right diagram*). *Gly* glycosylated; *ungly* unglycosylated. Data represent three independent experiments and error bars denote standard deviation. (**c**) Overexpression of Iso T1 C335S mutant increases K7 protein expression. ECV cells were transfected with plasmids as indicated. At 36 h post-transfection, whole cell lysates were prepared and analyzed by immunoblot with anti-Flag (K7, *top panel*), anti-HA (Iso T1C335S, *middle panel*), and anti-actin (*bottom panel*). (**d**) Overexpression of Iso T1 C335S inhibits K7 degradation. ECV cell transfection, pulse chase, autoradiography analysis were performed as described in (**b**). Data represent three independent experiments and error bars denote standard deviation.

Knockdown of Iso T1 Induces an Accumulation of Polyubiquitinated K7 Proteins

Previous data indicated that Iso T1 and its yeast homolog Ubp14 are important for cellular ubiquitin recycling and proteasome-dependent degradation of a model substrate, ub-P-βgal (23,24). The ub-P-βgal is a cytosolic soluble substrate of the end-rule pathway, while K7 is an ER membrane protein that is presumably degraded *via* the ERAD pathway. Given that knockdown of Iso T1 impeded the degradation of K7 and Iso T1 is involved in ubiquitin catabolism, we sought to examine whether Iso T1 is important for the ubiquitination of K7 that precedes the proteasomal degradation. Therefore, K7 ubiquitination was assessed in ECV cells by immunoprecipitation and immunoblot. When Iso T1 expression was reduced by shRNA-mediated silencing, significantly more polyubiquitinated K7 intermediates were detected (Fig. 8a). This result indicates that Iso T1 is important for K7 ubiquitination.

Iso T1 and yeast Ubp14 are proposed to disassemble polyubiquitin chains that otherwise may "saturate" proteasome ubiquitin acceptors. Thus, knockout of Ubp14 inhibits ubiquitin-dependent proteolysis (23). If such a defect in ubiquitin-dependent proteolysis of a proteasome substrate is solely due to a competitive binding of accumulated free polyubiquitin chains to ubiquitin acceptors of the proteasome, inhibition of the proteasome likely alleviates the accumulation of polyubiquitinated K7 when Iso T1 expression is reduced by shRNA-mediated silencing. To test this, K7 ubiquitination status was examined after Iso T1 knockdown and treatment by a proteasome inhibitor, lactacystin. Interestingly, the polyubiquitinated K7 was significantly increased even after treatment with lactacystin (Fig. 8b). These observations suggest that the accumulation of polyubiquitinated K7 is mainly due to increased ubiquitination, particularly when the proteasome is inhibited by lactacystin. These findings reveal that the disassembly of ubiquitin chains by Iso T1 is important for K7 ubiquitination.

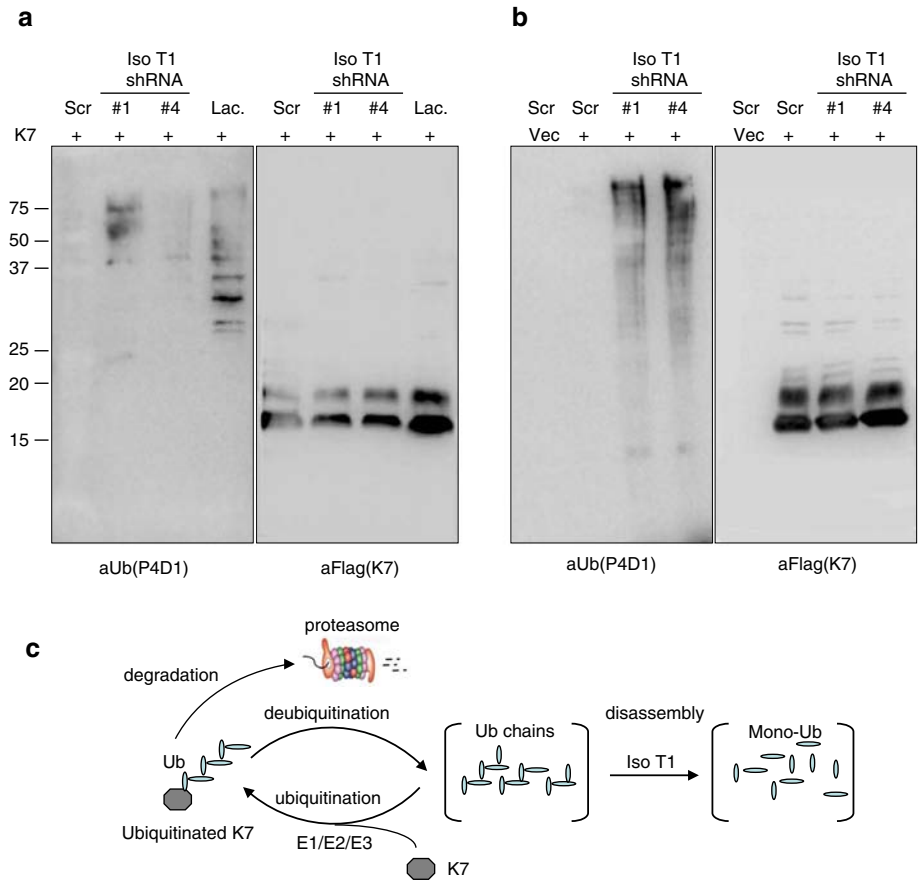

Fig. 8 Knockdown of Iso T1 induces accumulation of polyubiquitinated K7. (**a**) Knockdown of Iso T1 increases polyubiquitinated K7. ECV cells were transfected with plasmids as indicated. At 36 h post-transfection, cells were harvested and centrifuged cell lysates were precipitated with anti-Flag (K7) and eluted with the Flag peptide. Proteins were analyzed by immunoblot with anti-ubiquitin (*left panel*) and anti-Flag (K7, *right panel*). *Lac* Lactacystin. (**b**) Knockdown of Iso T1 increases polyubiquitinated K7 after treatment with a proteasome inhibitor, lactacystin. ECV cells were transfected with plasmids as indicated and treated with lactacystin (20 μM) for 6 h before harvest. Precipitation and immunoblot analysis were performed as described in (**a**). Proteins were analyzed by immunoblot with anti-ubiquitin (*left panel*) and anti-Flag (K7, *right panel*). (**c**) Model for Iso T1 function in K7 ubiquitination and degradation. Iso T1 disassembles free ubiquitin chain to prevent "clogging" of the proteasome and facilitates K7 degradation.

DISCUSSION

We have previously shown that K7 interacts with and induces vGPCR degradation, thereby reducing vGPCR tumorigenicity in nude mice (20). These findings implicate K7-regulated vGPCR expression in KSHV-associated malignancies. The K7 protein level is primarily regulated by protein degradation, therefore we set out to investigate the mechanisms by which K7 is degraded. Within this report, we demonstrated that K7 physically interacts with Iso T1 and induces an accumulation of ubiquitin chains in the membrane fraction. Using K7 as a substrate of the ERAD pathway, the knockdown of Iso T1 or overexpression of its enzyme dead mutant significantly inhibit K7 degradation and increase its protein expression. Interestingly, knockdown of Iso T1 also drastically increases K7 ubiquitination. These data support the notion that the disassembly of free ubiquitin chains is an important regulatory step of the ERAD pathway.

A proteomic screen identified ubiquitin chains accumulated in the membrane fraction derived from BJAB/K7 cells, which is further supported by immunoblot analysis using anti-ubiquitin antibody. Interestingly, these ubiquitin chains are not attached to protein substrates, indicative of altered ubiquitin catabolism. However, the free ubiquitin pool appears to be normal in the whole cell lysate (Fig. 2a), suggesting that K7 may specifically modulate membrane-associated polyubiquitin breakdown. Ubiquitin shows significant localization to the perinuclear region that is reminiscent of the ER and nuclear membrane, supporting its active role in the ERAD pathway. Upon K7 expression, ubiquitin displayed a punctate pattern that was shared by K7 staining (Fig. 2b). These punctate structures likely represent subcellular compartments where active protein degradation was shown to take place (29). Furthermore, K7 was detected in complexes precipitated by an anti-ubiquitin antibody (Fig. 2c). Conversely, ubiquitin was also identified by mass spectrometry as one of the K7-binding proteins (Fig. 2d). These data

indicate that K7 directly interacts with free polyubiquitin chains. However, K7 may recruit polyubiquitin chains to intracellular membranes through other indirect mechanisms, because K7 protein in the membrane fraction (of BJAB/K7 stable cells) is below detection in the absence of a proteasome inhibitor (data not shown). Nevertheless, these findings support the conclusion that K7 meddles the ubiquitin catabolism to induce its own protein degradation.

Iso T1 is one of the major cytosolic DUBs in mammalian cells. Deletion of UBp14 that encodes the yeast homolog of Iso T1 resulted in accumulation of free (unanchored) ubiquitin chains, a phenotype that we observed within the membrane fraction in cells expressing K7. This shared phenotype prompted us to investigate the deregulation of K7 by Iso T1. Indeed, K7 interacts with and increases the membrane association of Iso T1 and the overall DUB activity associated with the membrane fraction (Figs. 3 and 5). Consistent with a previous report (23), we observed delayed degradation kinetics of K7 upon Iso T1 knockdown (Fig. 7). Paradoxically, knockdown of Iso T1 led to a significant increase in K7 ubiquitination and interestingly, knockdown of Iso T1 increased K7 ubiquitination when proteasome activity was inhibited by lactacystin (Fig. 8b). Overexpression of Ubp14 also inhibited the ubiquitin-dependent proteolysis of ub-P-βgal, which is potentially due to reduced levels of free ubiquitin chains and consequent ubiquitination (23). If so, how does increased ubiquitination by Iso T1 knockdown contribute to reduced K7 degradation? The apparent paradox can be explained by the fact that proteasome degradation is downstream of the ubiquitination step. It is also possible that Iso T1 knock down promotes the ubiquitination/degradation the entire cellular protein repertoire causing a "traffic jam" of the proteasome degradation pathway and K7 accumulation. We have noticed that knocking down Iso T1 increased the protein expression of vGPCR and induced the accumulation of polyubiquitinated vGPCR (data not shown). Thus, the proteasome proteolytic activity will dictate the K7 degradation rate. Critical experiments will be those aimed to identify ERAD proteins that allow us to separate the positive effect on ubiquitination from the inhibitory effect on protein degradation upon Iso T1 knockdown. Additionally, experiments to examine the regulation of Iso T1 DUB activity in concert with other components of the ERAD pathway will reveal additional molecular details of K7 protein degradation.

The polyubiquitinated intermediates of K7 were significantly increased when Iso T1 expression was reduced and was independent of proteasome inhibition by lactacystin, suggesting that degradation of ubiquitinated K7 is very efficient and ubiquitination likely is one of the upstream rate-limiting steps. Such a conjecture is consistent with the observed specificity and degradation kinetics determined by various E3 ligase complexes of the ERAD pathway (30,31). So, how does Iso T1 DUB activity contribute to efficient ubiquitination? One intriguing possibility is that the Iso T1 DUB activity within membrane proximity shortens the long polyubiquitin chains and accumulate relative shorter (Ub3, Ub4, and Ub5) chains that can be directly conjugated to K7 and other ERAD substrates (Fig. 8c). By doing so, efficient ubiquitination is achieved to accelerate the ERAD of membrane proteins such as K7. It has been reported that an E2 (Ube2g2) in conjunction with gp78 (E3) directly transfers preformed ubiquitin chains to an ERAD substrate (32). It will be interesting to examine whether K7 degradation depends on the Ube2g2/gp78 ligase complex. Additionally, upstream molecular events such as substrate selection within the ER lumen likely represent other rate-limiting steps of ERAD pathway. One notable example is the exploitation of ERAD pathway by multiple herpesviral proteins to induce degradation of the class I major histocompatibility molecule (33–35).

Given that vGPCR is implicated in KSHV-associated malignancies, the regulated degradation of vGPCR induced by K7 will allow characterization of the molecular events that determine vGPCR protein level by the UPS system. This will also elucidate general mechanisms of how vGPCR-dependent transformation can be regulated by other viral factors and cellular pathways. These mechanisms may be exploited by other herpesviral GPCRs that are encoded by cytomegalovirus and Epstein-Barr virus. Furthermore, K7 is an early lytic gene product during KSHV infection and its expression is sustained in reactivated PEL cells. Although the roles of K7 in KSHV lytic replication are still unknown, the ability of K7 to regulate protein expression at a post-translational level in the ER compartment has significant implications for KSHV lytic replication. It is conceivable that K7 may induce other viral protein degradation in the ER compartment, thereby regulating viral lytic replication at a post-translational step. Actually, KSHV latent infected BCBL-1/T-Rex_K7 cells (K7 induced-expressing BCBL-1 cells)were used to analyze KSHV protein expression regulated by K7 and we found that K7 expression downregulates the protein expression of K1, K8.1, vIRF and K8 during KSHV lytic replication (data not shown). In fact, it is established that viral replication proceeds with cascades of gene expression regulated mainly at the transcription and translation level, yet very little is known how posttranslational mechanisms contribute to the highly programmed expression of viral proteins. K7 offers a potential system to investigate the post-translational events that modulate viral lytic replication.

In support of the importance of DUBs in viral infection, Kattenhorn *et al.* have identified a functional viral DUB, the N-terminal fragment of a large herpesvirus tegument protein (ORF64 of KSHV) that is conserved among all herpesvirus members (36,37). Combined with biochemical assays, a bioinformatics approach identified EBV thymidine kinase (BXLF1) and primase (BSLF1) that contain low yet significant intrinsic DUB activity (38). These studies echo the

notion that DUB enzymes are important for herpesvirus replication. With diverse cellular DUBs available during viral infection, herpesviruses likely have evolved strategies to usurp these critical components of the UPS pathway to regulate protein degradation and signal transduction (39). In fact, herpes simplex virus ICP0 engages cellular USP7 in order to increase ICP0 protein expression during viral infection (40), while Epstein-Bar virus EBNA1 targets USP7 to foster p53 degradation (41). Our current study demonstrated that K7 deregulates Iso T1 to induce an accumulation of free ubiquitin chains and promote protein ubiquitination, leading to rapid protein degradation. Future experiments will address the roles of K7-Iso T1 interaction in K7-induced protein degradation (such as K7 and vGPCR) and KSHV lytic replication.

ACKNOWLEDGMENTS AND DISCLOSURES

Jun Xiao and Hui Wu contributed equally to this work. This work was supported by the National Natural Science Foundation of China (81171583 & 31272634), Program for New Century Excellent Talents in University (NCET-11-0971) and the Funds of Hunan Province (12JJ1005 & 12A088).

REFERENCES

1. Chang Y, Cesarman E, Pessin MS, Lee F, Culpepper J, Knowles DM, *et al.* Identification of herpesvirus-like DNA sequences in AIDS-associated Kaposi's sarcoma. Science. 1994;266:1865–9.
2. Nador RG, Cesarman E, Knowles DM, Said JW. Herpes-like DNA sequences in a body-cavity-based lymphoma in an HIV-negative patient. N Engl J Med. 1995;333:943.
3. Soulier J, Grollet L, Oksenhendler E, Cacoub P, Cazals-Hatem D, Babinet P, *et al.* Kaposi's sarcoma-associated herpesvirus-like DNA sequences in multicentric Castleman's disease. Blood. 1995;86:1276–80.
4. Alexander L, Denekamp L, Knapp A, Auerbach MR, Damania B, Desrosiers RC. The primary sequence of rhesus monkey rhadinovirus isolate 26–95: sequence similarities to Kaposi's sarcoma-associated herpesvirus and rhesus monkey rhadinovirus isolate 17577. J Virol. 2000;74:3388–98.
5. Russo JJ, Bohenzky RA, Chien MC, Chen J, Yan M, Maddalena D, *et al.* Nucleotide sequence of the Kaposi sarcomaassociated herpesvirus (HHV8). Proc Natl Acad Sci U S A. 1996;93:14862–7.
6. Virgin 4th HW, Latreille P, Wamsley P, Hallsworth K, Weck KE, Dal Canto AJ, *et al.* Complete sequence and genomic analysis of murine gammaherpesvirus 68. J Virol. 1997;71:5894–904.
7. Damania B. Oncogenic gamma-herpesviruses: comparison of viral proteins involved in tumorigenesis. Nat Rev Microbiol. 2004;2:656–68.
8. Cesarman E, Mesri EA, Gershengorn MC. Viral G protein-coupled receptor and Kaposi's sarcoma: a model of paracrine neoplasia? J Exp Med. 2000;191:417–22.
9. Hayward GS. Initiation of angiogenic Kaposi's sarcoma lesions. Cancer Cell. 2003;3:1–3.
10. Chugh P, Matta H, Schamus S, Zachariah S, Kumar A, Richardson JA, *et al.* Constitutive NF-kappaB activation, normal Fas-induced apoptosis, and increased incidence of lymphoma in human herpes virus 8 K13 transgenic mice. Proc Natl Acad Sci U S A. 2005;102:12885–90.
11. Matta H, Chaudhary PM. Activation of alternative NF-kappa B pathway by human herpes virus 8-encoded Fasassociated death domain-like IL-1 beta-converting enzyme inhibitory protein (vFLIP). Proc Natl Acad Sci U S A. 2004;101:9399–404.
12. Montaner S, Sodhi A, Molinolo A, Bugge TH, Sawai ET, He Y, *et al.* Endothelial infection with KSHV genes *in vivo* reveals that vGPCR initiates Kaposi's sarcomagenesis and can promote the tumorigenic potential of viral latent genes. Cancer Cell. 2003;3:23–36.
13. Arvanitakis L, Geras-Raaka E, Varma A, Gershengorn MC, Cesarman E. Human herpesvirus KSHV encodes a constitutively active G-protein-coupled receptor linked to cell proliferation. Nature. 1997;385:347–50.
14. Bais C, Santomasso B, Coso O, Arvanitakis L, Raaka EG, Gutkind JS, *et al.* G-protein-coupled receptor of Kaposi's sarcomaassociated herpesvirus is a viral oncogene and angiogenesis activator. Nature. 1998;391:86–9.
15. Holst PJ, Rosenkilde MM, Manfra D, Chen SC, Wiekowski MT, Holst B, *et al.* Tumorigenesis induced by the HHV8-encoded chemokine receptor requires ligand modulation of high constitutive activity. J Clin Invest. 2001;108:1789–96.
16. Krishnan HH, Naranatt PP, Smith MS, Zeng L, Bloomer C, Chandran B. Concurrent expression of latent and a limited number of lytic genes with immune modulation and antiapoptotic function by Kaposi's sarcoma-associated herpesvirus early during infection of primary endothelial and fibroblast cells and subsequent decline of lytic gene expression. J Virol. 2004;78:3601–20.
17. Wang HW, Sharp TV, Koumi A, Koentges G, Boshoff C. Characterization of an anti-apoptotic glycoprotein encoded by Kaposi's sarcoma-associated herpesvirus which resembles a spliced variant of human survivin. EMBO J. 2002;21:2602–15.
18. Feng P, Park J, Lee BS, Lee SH, Bram RJ, Jung JU. Kaposi's sarcoma-associated herpesvirus mitochondrial K7 protein targets a cellular calcium-modulating cyclophilin ligand to modulate intracellular calcium concentration and inhibit apoptosis. J Virol. 2002;76:11491–504.
19. Feng P, Scott CW, Cho NH, Nakamura H, Chung YH, Monteiro MJ, *et al.* Kaposi's sarcoma-associated herpesvirus K7 protein targets a ubiquitin-like/ubiquitin-associated domain-containing protein to promote protein degradation. Mol Cell Biol. 2004;24:3938–48.
20. Feng H, Dong X, Negaard A, Feng P. Kaposi's sarcoma-associated herpesvirus K7 induces viral G protein-coupled receptor degradation and reduces its tumorigenicity. PLoS Pathog. 2008;4:e1000157.
21. Komander D, Rape M. The ubiquitin code. Annu Rev Biochem. 2012;81:203–29.
22. Leggett DS, Hanna J, Borodovsky A, Crosas B, Schmidt M, Baker RT, *et al.* Multiple associated proteins regulate proteasome structure and function. Mol Cell. 2002;10:495–507.
23. Amerik A, Swaminathan S, Krantz BA, Wilkinson KD, Hochstrasser M. *In vivo* disassembly of free polyubiquitin chains by yeast Ubp14 modulates rates of protein degradation by the proteasome. EMBO J. 1997;16:4826–38.
24. Wilkinson KD, Tashayev VL, O'Connor LB, Larsen CN, Kasperek E, Pickart CM. Metabolism of the polyubiquitin degradation signal: structure, mechanism, and role of isopeptidase T. Biochemistry. 1995;34:14535–46.
25. Nakamura H, Lu M, Gwack Y, Souvlis J, Zeichner SL, Jung JU. Global changes in Kaposi's sarcoma-associated virus gene expression patterns following expression of a tetracyclineinducible Rta transactivator. J Virol. 2003;77:4205–20.

26. Feng P, Liang C, Shin YC, Xiaofei E, Zhang W, Gravel R, *et al.* A novel inhibitory mechanism of mitochondrion-dependent apoptosis by a herpesviral protein. PLoS Pathog. 2007;3:e174.
27. Trompouki E, Hatzivassiliou E, Tsichritzis T, Farmer H, Ashworth A, Mosialos G. CYLD is a deubiquitinating enzyme that negatively regulates NF-kappaB activation by TNFR family members. Nature. 2003;424:793–6.
28. Nijman SM, Luna-Vargas MP, Velds A, Brummelkamp TR, Dirac AM, Sixma TK, *et al.* A genomic and functional inventory of deubiquitinating enzymes. Cell. 2005;123:773–86.
29. Kaganovich D, Kopito R, Frydman J. Misfolded proteins partition between two distinct quality control compartments. Nature. 2008;454:1088–95.
30. Carvalho P, Goder V, Rapoport TA. Distinct ubiquitin-ligase complexes define convergent pathways for the degradation of ER proteins. Cell. 2006;126:361–73.
31. Denic V, Quan EM, Weissman JS. A luminal surveillance complex that selects misfolded glycoproteins for ERassociated degradation. Cell. 2006;126:349–59.
32. Li W, Tu D, Brunger AT, Ye Y. A ubiquitin ligase transfers preformed polyubiquitin chains from a conjugating enzyme to a substrate. Nature. 2007;446:333–7.
33. Van der Veen AG, Ploegh HL. Ubiquitin-like proteins. Annu Rev Biochem. 2012;81:323–57.
34. Lilley BN, Ploegh HL. Viral modulation of antigen presentation: manipulation of cellular targets in the ER and beyond. Immunol Rev. 2005;207:126–44.
35. Wang X, Ye Y, Lencer W, Hansen TH. The viral E3 ubiquitin ligase mK3 uses the Derlin/p97 endoplasmic reticulumassociated degradation pathway to mediate down-regulation of major histocompatibility complex class I proteins. J Biol Chem. 2006;281:8636–44.
36. Gredmark S, Schlieker C, Quesada V, Spooner E, Ploegh HL. A functional ubiquitin-specific protease embedded in the large tegument protein (ORF64) of murine gammaherpesvirus 68 is active during the course of infection. J Virol. 2007;81:10300–9.
37. Kattenhorn LM, Korbel GA, Kessler BM, Spooner E, Ploegh HL. A deubiquitinating enzyme encoded by HSV-1 belongs to a family of cysteine proteases that is conserved across the family Herpesviridae. Mol Cell. 2005;19:547–57.
38. Sompallae R, Gastaldello S, Hildebrand S, Zinin N, Hassink G, Lindsten K, *et al.* Epstein-barr virus encodes three bona fide ubiquitin-specific proteases. J Virol. 2008;82(21):10477–86.
39. Isaacson MK, Ploegh HL. Ubiquitination, ubiquitin-like modifiers, and deubiquitination in viral infection. Cell Host Microbe. 2009;5(6):559–70.
40. Boutell C, Canning M, Orr A, Everett RD. Reciprocal activities between herpes simplex virus type 1 regulatory protein ICP0, a ubiquitin E3 ligase, and ubiquitin-specific protease USP7. J Virol. 2005;79:12342–54.
41. Saridakis V, Sheng Y, Sarkari F, Holowaty MN, Shire K, Nguyen T, *et al.* Structure of the p53 binding domain of HAUSP/USP7 bound to Epstein-Barr nuclear antigen 1 implications for EBV-mediated immortalization. Mol Cell. 2005;18:25–36.